Electronic Supplementary Material (ESI) for Physical Chemistry Chemical Physics.

Supplementary Information

Ultrafast Photoisomerization Mechanism of Azaborine Revealed by Nonadiabatic Molecular Dynamics Simulation

Sangmin Jeong,[a] Eunji Park,[b] Joonghan Kim[b,*] and Kyung Hwan Kim[a,*]

[a]Department of Chemistry, POSTECH, Pohang, 37673, Republic of Korea. E-mail: kimkyungwhan@postech.ac.kr

[b]Department of Chemistry, The Catholic University of Korea, Bucheon, 14662, Republic of Korea. E-mail: joonghankim@catholic.ac.kr

*Corresponding author

E-mail: joonghankim@catholic.ac.kr, kimkyunghwan@postech.ac.kr

S1. Active orbitals of azaborine in the SA3-CAS(6,6) calculation

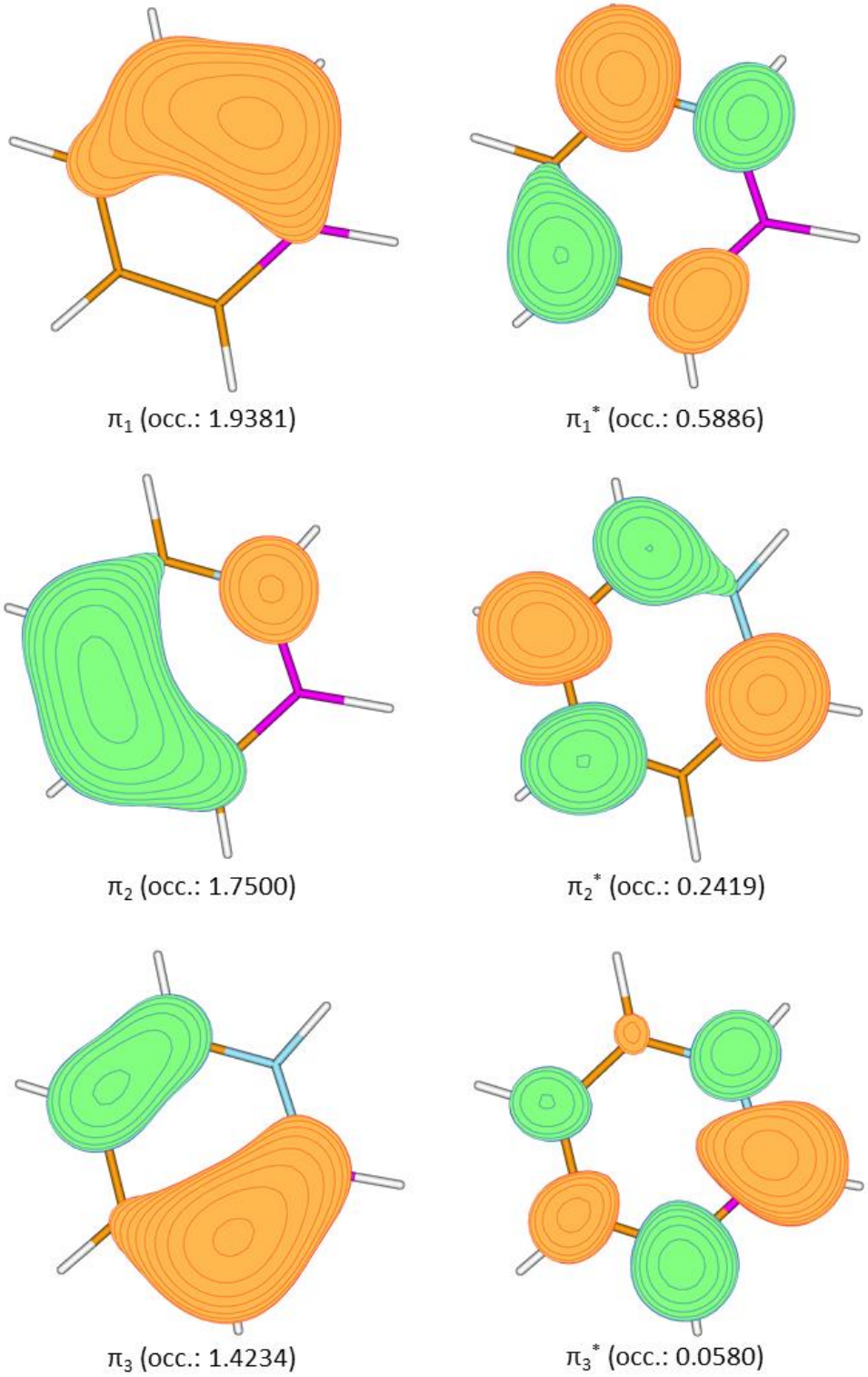

Fig S1. Active orbitals of azaborine in the planar structure, calculated with SA3-CAS(6,6)/ANO-RCC-VDZP level of theory. The molecular structure was optimized using ωB97XD/6-311++G(d,p). Orange, white, purple, and light blue sticks correspond to C, H, B, and N atoms, respectively.

S2. Sampling the initial trajectories for the TSH dynamics simulation

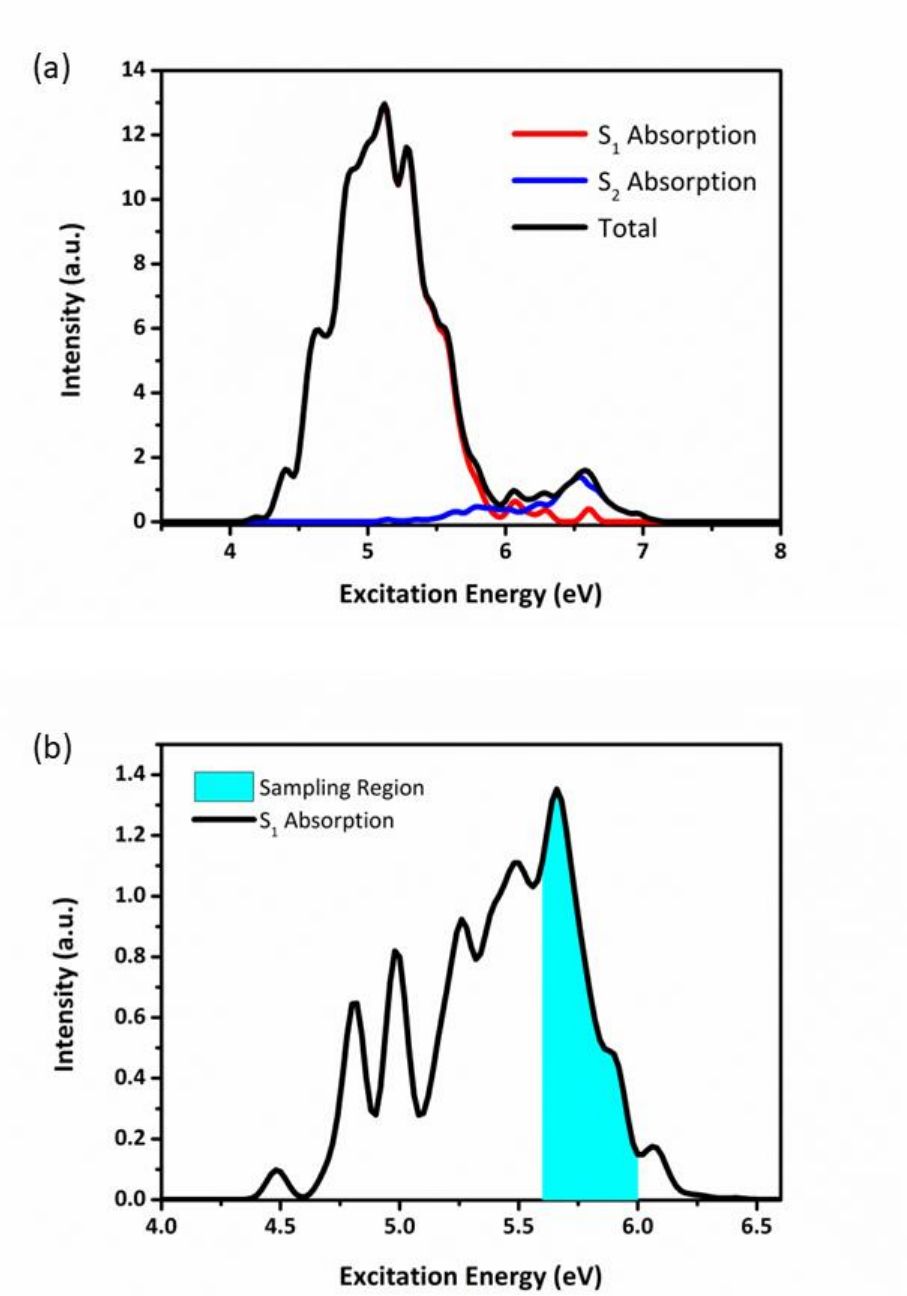

Fig S2. (a) Absorption spectrum (black) of azaborine calculated by the initial Wigner sampling with MS-CASPT2/ANO-RCC-VDZP level. Contributions both from $S_0 \rightarrow S_1$ excitation (red) $S_0 \rightarrow S_2$ excitation (blue) are considered. (b) Absorption spectrum (black) of azaborine calculated by the initial Wigner sampling with SA3-CAS(6,6)/ANO-RCC-VDZP level. Contribution only from $S_0 \rightarrow S_1$ excitation is used here. The excitation window from 5.6 eV to 6.0 eV indicated in cyan was selected for further simulations.

Table S1. The vertical transition energies (T_vs) in eV and the oscillator strengths (in parentheses) of $S_0 \rightarrow S_1$ and $S_0 \rightarrow S_2$ transitions calculated using the five different level of theory. For complete active space methods, the weights of each excitation character and their coefficients (in square brackets) are also noted.

T_V (f_{osc})	SA3-CAS(6,6)/ ANO-RCC-VDZP	SA3-CAS(6,6)/ ANO-RCC-VTZP	MS-CASPT2/ ANO-RCC-VDZP	MS-CASPT2/ ANO-RCC-VTZP	EOM-CCSD/ 6-311++G(d,p)
$S_0 \rightarrow S_1$	5.50 eV (0.1155)	5.46 eV (0.1189)	4.74 eV (0.1413)	4.57 eV (0.1423)	5.16 eV (0.1631)
	$\pi_3 \rightarrow \pi_4$ 29%	$\pi_3 \rightarrow \pi_4$ 31%	$\pi_3 \rightarrow \pi_4$ 50%	$\pi_3 \rightarrow \pi_4$ 52%	$\pi_3 \rightarrow \pi_4$ 80%
	[-0.5404]	[-0.5528]	[-0.7038]	[-0.7245]	
	$\pi_3 \rightarrow \pi_5$ 22%	$\pi_3 \rightarrow \pi_5$ 21%	$\pi_3 \rightarrow \pi_5$ 12%	$\pi_3 \rightarrow \pi_5$ 11%	
	[0.4656]	[0.4584]	[0.3500]	[0.3300]	
	$\pi_2 \rightarrow \pi_4$ 18%	$\pi_2 \rightarrow \pi_4$ 18%	$\pi_2 \rightarrow \pi_4$ 10%	$\pi_2 \rightarrow \pi_4$ 9%	
	[0.4270]	[-0.4250]	[0.3156]	[-0.3010]	
$S_0 \rightarrow S_2$	7.01 eV (0.0597)	6.93 eV (0.0617)	6.36 eV (0.0155)	6.16 eV (0.0132)	6.34 eV (0.0838)
	$\pi_3 \rightarrow \pi_4$ 39%	$\pi_3 \rightarrow \pi_4$ 39%	$\pi_3 \rightarrow \pi_4$ 23%	$\pi_3 \rightarrow \pi_4$ 21%	$\pi_3 \rightarrow \pi_5$ 72%
	[-0.6289]	[-0.6256]	[-0.4768]	[-0.4565]	
	$\pi_3 \rightarrow \pi_5$ 15%	$\pi_3 \rightarrow \pi_5$ 16%	$\pi_3 \rightarrow \pi_5$ 25%	$\pi_3 \rightarrow \pi_5$ 26%	$\pi_2 \rightarrow \pi_4$ 13%
	[-0.3915]	[-0.3999]	[-0.4973]	[-0.5112]	
	$\pi_2 \rightarrow \pi_4$ 15%	$\pi_2 \rightarrow \pi_4$ 16%	$\pi_2 \rightarrow \pi_4$ 24%	$\pi_2 \rightarrow \pi_4$ 25%	
	[-0.3909]	[0.3993]	[-0.4865]	[0.4998]	

Based the calculation result with MS-CASPT2/ANO-RCC-VDZP level, we could conclude that the contribution from $S_0 \rightarrow S_2$ transition is negligible under our simulation condition (See Table S1 and Fig S2(a)). Thus, only the S_1 state was set as the initial electronic state for all our simulations. The initial states in the 5.6 eV to 6.0 eV excitation window, shown in cyan color in Fig S2, were selected for further simulations. This sampling criterion is consistent with the condition in the previous experimental study.[1] They used 253.7 nm light for excitation, while the peak of the absorption spectrum of azaborine is at around 269 nm.[1]

S3. Time evolution of important geometry parameters for hydrogen dissociation pathway

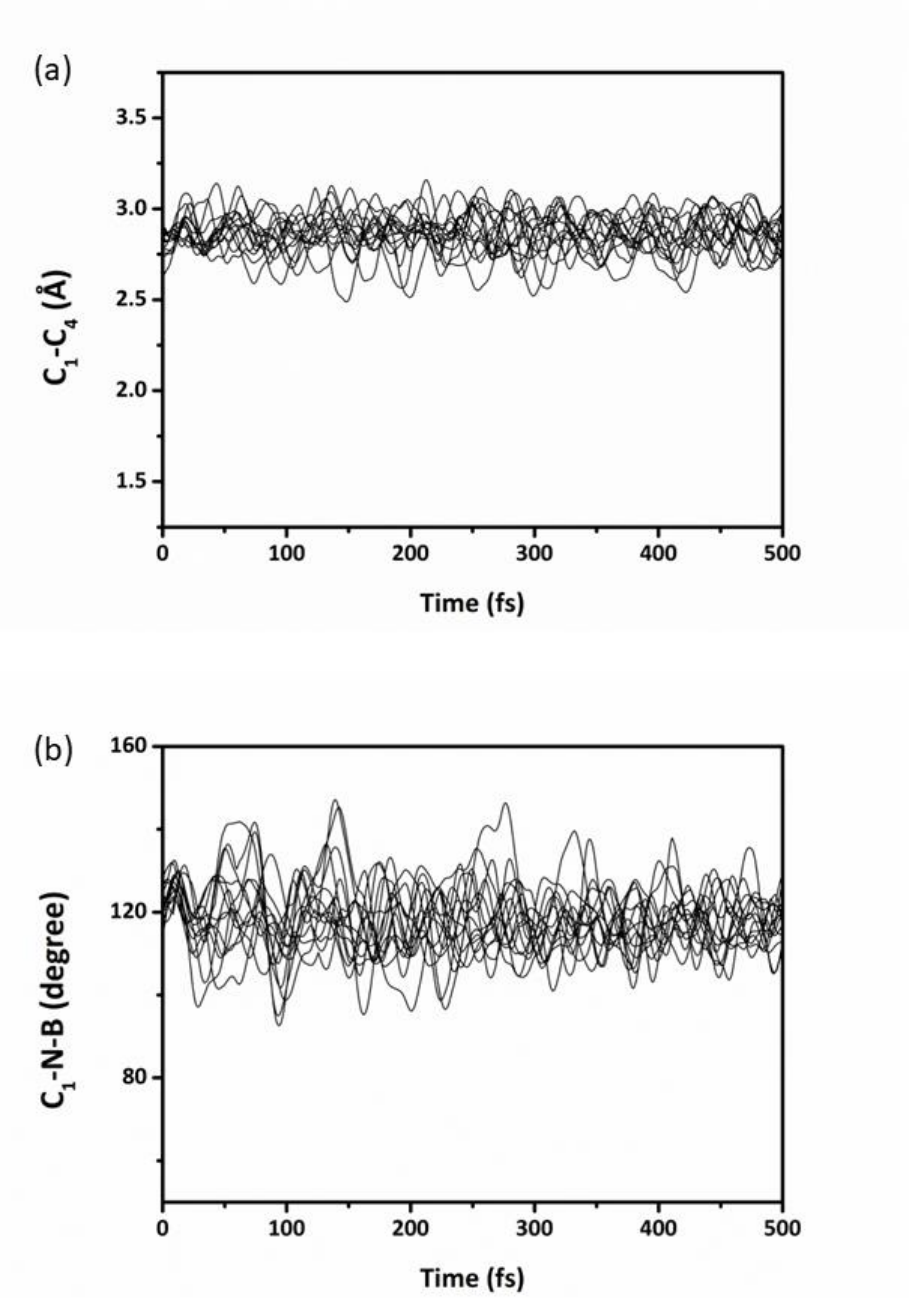

Fig S3. Ensemble plots for (a) C_1–C_4 distance and (b) C_1–N–B angle of trajectories that exhibit hydrogen dissociation.

S4. The second excited state of azaborine

We performed the geometry optimization starting from the FC region of the S_2 state to investigate its decay pathway of the S_2 state. Geometry optimization follows the ring puckering mode but could not find any stable local minima, due to the near degenerated region of S_2/S_1. At the end point of the geometry optimization, we perform the conical intersection optimization between the S_2 and S_1 states, which led to the S_2/S_1 MECP geometry without having any barrier between the FC region of S_2 and S_2/S_1 MECP. Similar to benzene,[2] the S_2 state of azaborine has a downward gradient at the FC region toward the Dewar-like distortion, and meets the S_1 state with a small displacement. Fig S4 shows the optimized structure at the S_2/S_1 MECP, together with the gradient difference vector (GDV) and the derivative coupling vector (DCV).

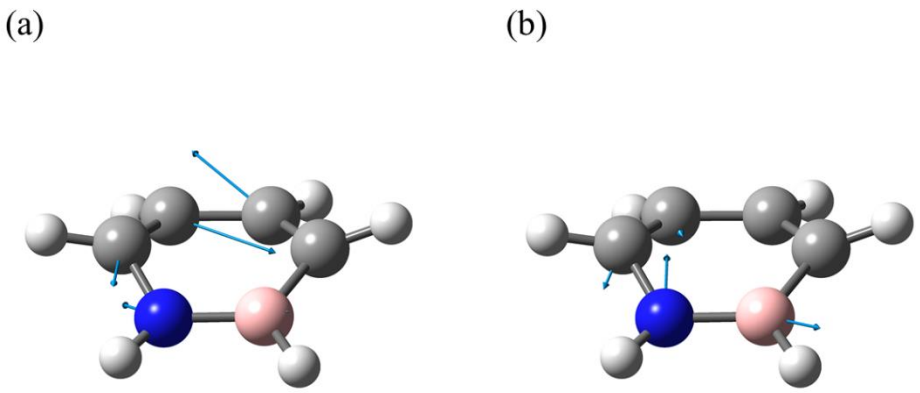

Fig S4. (a) GDV and (b) DCV are shown on the optimized S_2/S_1 MECP structure.

The energy gap between S_1 and S_2 of azaborine, estimated to be 1.5~1.6 eV according to Table S1 in all levels of theory, is smaller than that of benzene.[2] This small energy gap allows the two excited states to cross at the position close to the FC region, indicating that the S_2/S_1 MECP is barrierlessly connected to the FC region in the S_2 state. The small gap also explains the small population of the S_2 state at an early time in the simulation shown in Fig 1.

To find the relaxation pathway from the S_2 to the S_1 state, we introduced a slight perturbation of about 1 GDV to the S_2/S_1 MECP geometry and performed the geometry optimization in the S_1 state starting from this structure. This calculation also yields the region of near-degenerate energy between the S_1 and S_0 states, and we further optimized the MECP geometry between the S_1 and S_0 states. This calculation shows that the S_2/S_1 MECP is directly linked to the S_1/S_0 MECP. It indicates that unlike benzene,[2] the population in the S_2 state can undergo a decay process similar to the population in the S_1 state, suggesting that the initial $S_1 \rightarrow S_2$ transition in some of our trajectories does not have a significant effect.

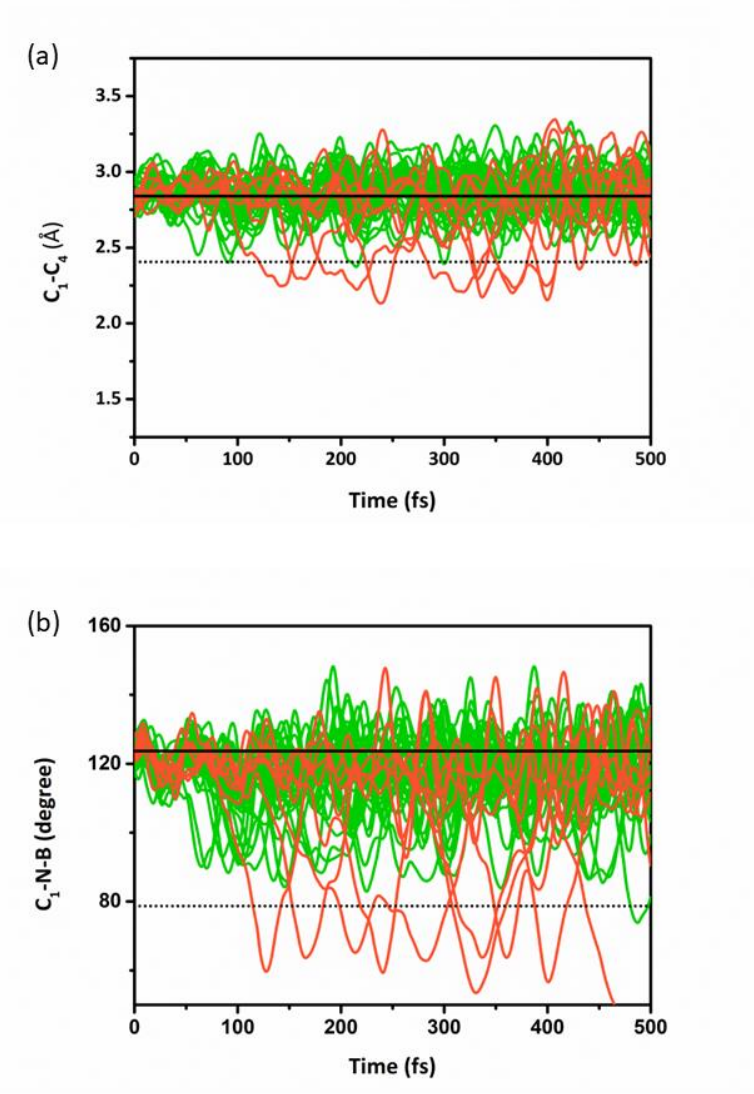

Fig S5. Ensemble plots for (a) C_1–C_4 bond distance and (b) C_1–N–B angle of the that involve the initial $S_1 \rightarrow S_2$ transition. The green and orange lines indicate the trajectories in path 1 and path 2, respectively. Representative geometric values from the planar reactant and prefulvene-like intermediate are indicated by solid and dotted horizontal lines. Atom indexing and geometrical parameters used in (a) and (b) are the same as the given in Fig 3.

S5. The representative plot of the dissociative pathway and the ring reformation path

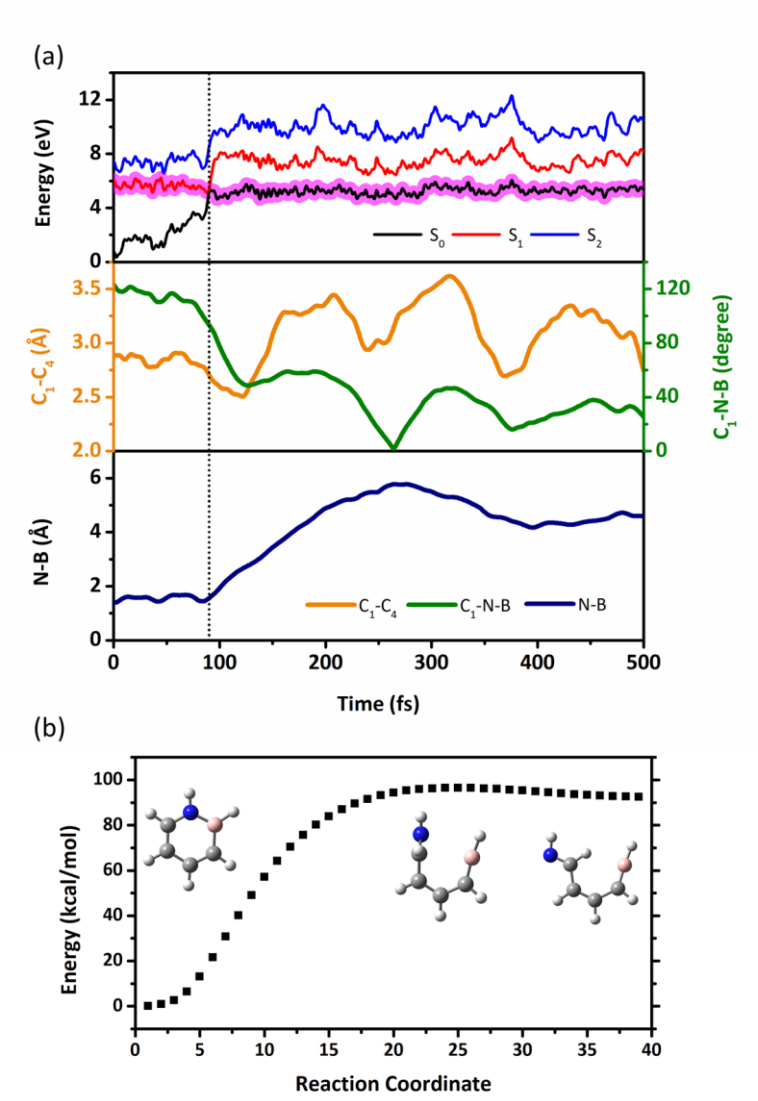

Fig S6. (a) Time-energy plot with geometry parameters of a representative trajectory of the pathway with B–N bond dissociation, and (b) reaction coordinate from the B–N dissociation chain to the planar ring form.

We calculated the relative energy following the reaction coordinate between the chain structure and the planar structure as shown in Fig S6. Since the energy barrier from the chain form to the planar form is very small, we expect that this dissociative trajectory can easily restore the ring structure.

S6. Theoretical estimation of photoconversion in continuous irradiation

Based on the quantum yield obtained from our NAMD simulation, the photoconversion rate and the total conversion time have been roughly estimated. We first calculated the absorption cross section of the molecule based on the excitation energy and the oscillator strength by using the following equation.[3]

$$\sigma = \pi e^2 / 2mc\varepsilon_0 (f_{osc} g(E - \Delta E_0, \delta)), g(E - \Delta E_0, \delta) = \hbar/(\delta\sqrt{2\pi}) * exp(-(E - \Delta E_0)^2 / 2\delta^2)$$

The obtained absorption cross section then allows us to calculate the probability of the absorption event from a single photon irradiation as follows.

$$A = \varepsilon bc = \sigma N_A/(ln(10) * 10^3) * b * c, T = 10^{-A}$$

Since some values of experimental parameters from the previous study such as the Hg lamp power and the molarity of the system are limited, we used approximate values by assuming reasonable experimental conditions. Our assumptions include a system consisting of 60 μM of azaborine, a 1:1000 ratio of azaborine to neon, inside a 1 cm cubic box, and being irradiated with 253.7 nm UV light with a power density of 0.1 mW/cm^2. We then simply calculated the time that is needed for the full conversion as follows.

$$Prob = (Power\ density(W/cm^2)) * (Number\ of\ photons\ in\ 1\ W\ of\ 253.7\ nm\ light) * (1 - T)$$

$$* (2\ traj\ /\ 82\ traj) = 0.0025\ \%/s$$

$$(Portion\ of\ isomer) = Prob * t, \qquad t_{full\ conversion} = 1/Prob = 3.4 * 10^4\ s$$

In our rough estimation, full photoconversion of azaborine can happen within about 570 min. It qualitatively showed that full conversion can be achieved within a reasonable time, which is consistent with the experimental observation even with a low quantum yield estimated from our simulation.

S7. XYZ coordinates of the optimized structures

Planar structure (S_0 minimum) optimized by ωB97XD/6-311++G(d,p)

C	1.05776700	-0.84978400	0.00003300
C	-1.18102700	0.87994000	0.00005000
C	-1.32610500	-0.48144400	0.00000400
C	-0.20414400	-1.35727900	0.00002600
H	1.93360500	-1.48846300	-0.00026200
H	2.23562700	0.79066200	-0.00003400
H	0.51616300	2.62041600	-0.00025100
H	-2.07910100	1.49022800	-0.00002900
H	-2.31532900	-0.93380200	-0.00019300
H	-0.34234000	-2.43075000	-0.00011600
B	0.21510900	1.46476600	-0.00002100
N	1.27098400	0.49704000	0.00004400

Prefulvene-like structure optimized by ωB97XD/6-311++G(d,p)

C	0.58832800	-0.64649700	0.50826600
C	-0.72025500	1.15577400	0.04382900
C	-1.50877900	-0.04396500	-0.13977600
C	-0.72274000	-1.12350100	0.01657500
H	0.86257900	-0.69177200	1.56265600
H	2.42295200	-0.24424200	-0.18583700
H	1.51999200	1.88658300	0.30288400
H	-1.19797700	2.08227000	0.35883200
H	-2.54188200	-0.04629300	-0.47248500
H	-0.86908500	-2.12739900	-0.36281200
B	0.75970200	1.04705600	-0.07264600
N	1.45508400	-0.30646900	-0.48762400

Dewar structure optimized by ωB97XD/6-311++G(d,p)

C	-0.06545600	0.68112700	0.55455000
C	0.09630900	-0.87955500	0.49799200
C	1.36430700	-0.57448000	-0.28246400
C	1.21630700	0.75355200	-0.25953200
H	-0.12297300	1.21231000	1.50558900
H	-1.84561100	1.36593500	-0.58732400
H	-2.03706200	-1.54383800	-0.87242700
H	0.17894000	-1.46355100	1.41474000
H	2.09650300	-1.23127600	-0.73884000
H	1.75115800	1.57970000	-0.71197500
B	-1.28427400	-0.79517900	-0.33193400
N	-1.32405500	0.59610700	-0.20191000

Chain structure optimized by ωB97XD/6-311++G(d,p)

C	1.16494700	-0.27044100	0.07484300
C	-1.86221700	-0.04513100	0.02767800
C	-0.91168000	1.05979600	-0.01357100
C	0.43140200	0.97910700	-0.00981500
H	0.55955800	-1.17395800	0.28157000
H	2.75949800	-1.29400300	0.05356400
H	-1.62175300	-2.58834200	-0.13980600
H	-2.91348500	0.23809400	0.12130700
H	-1.34999100	2.05216400	-0.06097400
H	1.03088400	1.88063300	-0.06510700
B	-1.68097400	-1.41948700	-0.05643500
N	2.42934900	-0.33673400	-0.05474100

TS between Chain and Planar structure optimized by ωB97XD/6-311++G(d,p)

C	-1.13709600	-0.18726600	0.41828500
C	1.60201800	0.44599900	0.02561200
C	1.11215900	-0.92024700	-0.12383900
C	-0.18151200	-1.23714400	0.01277300
H	-1.12325800	0.08263500	1.48639400
H	-2.47094800	1.09956900	0.05106500
H	0.32554500	2.66739700	-0.06296000
H	2.67661500	0.58481800	0.14772500
H	1.83002900	-1.69002400	-0.39033200
H	-0.55492100	-2.23603400	-0.18188900
B	0.83987400	1.61452300	-0.02106600
N	-1.89369200	0.40156600	-0.42023800

Minimum energy crossing point (MECP) between S_2 and S_1 optimized by SA3-CAS(6,6)/ 6-311++G(d,p)

C	-0.63277415	-1.16512333	0.29970247
C	0.72422924	1.26232215	0.24350732
C	-0.75595696	1.27861525	0.14282717
C	-1.46185558	0.05024109	0.13060949
H	-1.09181293	-2.11745689	0.48784091
H	1.00040794	-2.07262957	-0.57018491
H	2.60356825	-0.09037946	-0.50721034
H	1.21828462	2.13368111	0.63406955
H	-1.27410976	2.20125800	-0.05333212
H	-2.46490388	-0.01992488	-0.25224836
B	1.45002580	-0.02138553	-0.21984880
N	0.63365540	-1.18512094	-0.30965338

References

1. A. Chrostowska, S. Xu, A. N. Lamm, A. Mazière, C. D. Weber, A. Dargelos, P. Baylère, A. Graciaa and S.-Y. Liu, *J. Am. Chem. Soc.*, 2012, **134**, 10279-10285.
2. I. J. Palmer, I. N. Ragazos, F. Bernardi, M. Olivucci and M. A. Robb, *J. Am. Chem. Soc.*, 1993, **115**, 673-682.
3. M. Barbatti, A. J. A. Aquino and H. Lischka, *Phys. Chem. Chem. Phys.*, 2010, **12**, 4959-4967.